IEEE Photonics Journal
An IEEE Photonics Society Publication

Open Access

Optofluidic Tunable Linear Narrow-Band Filter Based on Bragg Nanocavity

Volume 9, Number 2, April 2017

Chaolong Fang
Bo Dai
Qiao Xu
Qi Wang
Dawei Zhang

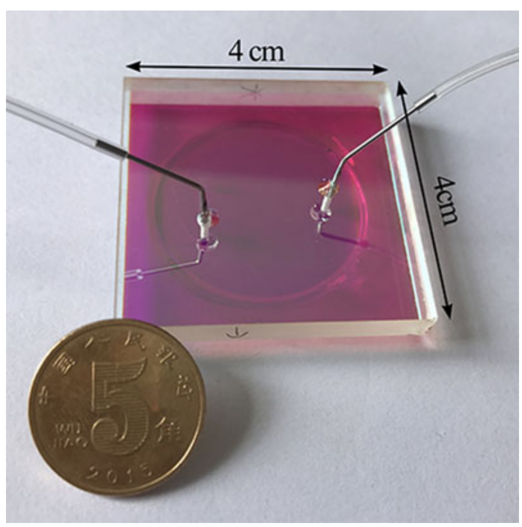

DOI: 10.1109/JPHOT.2017.2655005
1943-0655

Optofluidic Tunable Linear Narrow-Band Filter Based on Bragg Nanocavity

Chaolong Fang, Bo Dai, Qiao Xu, Qi Wang, and Dawei Zhang

Engineering Research Center of Optical Instrument and System, The Ministry of Education, Shanghai Key Laboratory of Modern Optical Systems, University of Shanghai for Science and Technology, Shanghai 200093, China

DOI:10.1109/JPHOT.2017.2655005

Manuscript received December 16, 2016; revised January 13, 2017; accepted January 15, 2017. Date of publication January 18, 2017; date of current version February 24, 2017. This work was supported in part by the National Key Research and Development Program of China (2016YFD0500603), in part by the National Basic Research Program of China (973 Program) (2015CB352001), in part by the Yangtze River Delta Joint Project of Shanghai Science and Technology Commission (16395810500), and in part by the Innovation Program of the Shanghai Municipal Education Commission (15ZZ071).
Corresponding author: D. Zhang (e-mail: dwzhang@usst.edu.cn).

Abstract: A compact, tunable linear optofluidic Bragg filter is simulated, designed, fabricated, and characterized. The device consists of a nanocavity sandwiched by two symmetrical film stacks made of high- and low-refractive-index dielectric materials. The fabrication parameters are simulated by using the commercial software Essentical Macleod. The resonant wavelength can be linearly shifted by up to 34.8 nm when the refractive index of the liquid injected into the Bragg nanocavity varies from 1.333 to 1.51. Meanwhile, the filter has a narrow bandwidth of 1.1 nm and a very high extinction ratio of –20.2 dB with the sensitivity ($\Delta\lambda/\Delta n$) of 374 nm/RIU.

Index Terms: Tunable filters, fabrication and characterization, nanocavities, photonic crystals.

1. Introduction

Photonic crystals, the dielectric refractive index of which periodically changes in space, were first defined by Yablonovitch [1] and John [2] in 1987. Since then, an increasing number of researchers have shown great interest in photonic crystals. The periodic structure of photonic crystals can generate a photonic bandgap in which the propagation of electromagnetic waves is prohibited. Electromagnetic waves with frequencies in the photonic bandgap can be reflected with a high efficiency by photonic crystal materials, which is useful for many applications including dielectric mirrors and optical filters [3], [4].

An ultra-narrow band transmission filter, also known as a Bragg filter, can be realized by inserting a multilayer dielectric film stack, as a simple 1-D photonic crystal structure, into a dielectric layer, which breaks the periodic structure. The characteristics of the reflection spectrum of the Bragg filter are closely related to the properties of the defect layer, such as its refractive index and thickness. The quality of the transmission peak in the band gap and the resonant wavelength are dependent on the donor impurity concentration of n-Ge and the thickness of the defect layer [5].

Many researchers have attempted to realize a tunable Bragg filter consisting of a periodic dielectric film by changing the thickness and refractive index of the defect layer. For instance, piezo-

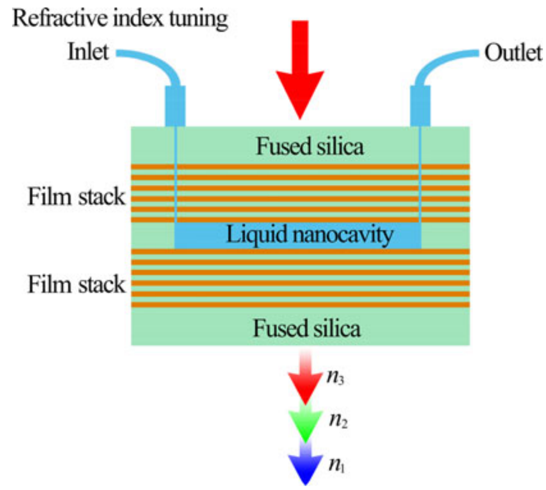

Fig. 1. Schematic of the proposed refractive-index-sensitive optofluidic Bragg filter.

electric materials [6], doped semiconductors [7], magnetic materials [8], liquid crystals [9], and phase-change materials [10] were used as defect layers to tune the resonant wavelength. Recently, our research group fabricated a wedge-shaped defect layer by using the ion-beam etching method, in which the resonant wavelength varied as a function of spatial position [11].

Over the last two decades, optofluidics has integrated photonics into microfluidic systems and presents new possibilities for developing lab-on-a-chip (LOC) devices. Optofludic systems have been demonstrated to show excellent performance, including high sensitivity, reconfigurable capability, and compactness [12]–[14]. Due to the combination of photonics and microfluidics, many optofluidic devices have been developed with powerful tunability, such as tunable gratings [15], [16], tunable diffraction gratings [16], variable optical attenuators [17], tunable guided-mode resonance filters [18], tunable microlenses [19], and tunable limiting devices [20].

Recently, some optical filter integrated optofluidics technology have been present, such as anti-resonant reflecting optical waveguide [21], [22], liquid-crystal microflows [23], and optofluidic Bragg filters [24]–[26]. The performance of the Bragg filters based on 1-D photonic crystal has two criteria: 1) narrow linewidth and 2) high extinction ratio. Narrow linewidth and high extinction ratio are preferred for high resolution and high signal-to-noise ratio. However, narrow bandwidth and high extinction ratio are not always available in the optofluidic filtering devices [27], [28]. In this paper, an optofluidic Bragg nanocavity filter consisting of periodic multilayer dielectric films is designed and fabricated. The designed filter can realize a narrow bandwidth of approximately 1.1 nm and remarkably improve the extinction ratio.

2. Operation Principle

In the designed tunable optofluidic Bragg filter, alternate Ta_2O_5 and SiO_2 films can be expressed as $(BA)^N$ $BDB(AB)^N$, where D is the liquid defect layer and $(AB)^N$ is the host photonic crystal with A and B being the high- and low-refractive-index layers, respectively, and N being the stack number. The structure is shown in Fig. 1. A nanocavity is sandwiched by two fused-silica substrates with a multilayer dielectric film stack. An inlet and an outlet locate on the top of the filter. A liquid injected into the nanocavity functions as a defect layer and breaks the one-dimensional periodic-photonic-crystal structure. A narrow-band transmission filter can be realized and the resonant wavelength can be shifted with the change of the refractive index of the liquid. The resonant wavelength can be

3. Optofluidic Bragg filter

3.1 Design of optofluidic Bragg filter

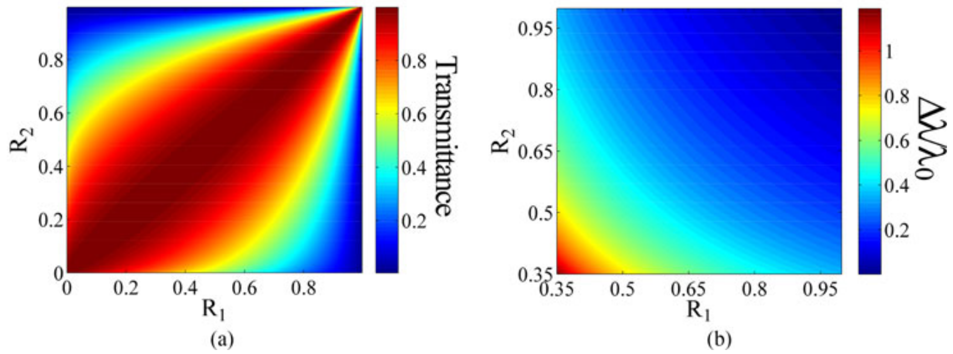

Fig. 2. (a) Transmittance and (b) bandwidth of the resonant spectrum with respect to the reflectivity of the Bragg layers above and below the defect layer.

confirmed according to the phase-matching condition, which is expressed as follows [29], [30]:

$$\lambda_0 = \frac{2\pi n d}{(2k+1)\pi - (\varphi_1 + \varphi_2)} = \frac{2\pi n d}{m}$$
$$m = (2k+1)\pi - (\varphi_1 + \varphi_2)\ , \quad k = 0, \pm 1, \pm 2, \ldots \tag{1}$$

where n and d are the refractive index and thickness of the defect layer. m is the phase of the defect layer and k is an integer. φ_1 and φ_2 are the phases of the Bragg layers above and below the defect layer, respectively. According to (1), the resonant wavelength varies with change of the refractive index when the film structure is determined. Accordingly, the resonant wavelength changes if the liquid of different refractive index is injected into the nanocavity.

3. Optofluidic Bragg Filter

3.1 Design of Optofluidic Bragg Filter

The resonant transmittance and bandwidth are related to the reflectivity of the upper and following interfaces of the defect layer. Per Macleod's theory [21], the transmittance and the ratio between the full-width-at-half-maximum bandwidth (linewidth) and resonant wavelength depend on the reflectivity of the Bragg layers above and below the defect layer and are expressed as follows [29], [30]:

$$\mathrm{T} = \frac{(1-R_1)(1-R_2)}{\left(1-\sqrt{R_1 R_2}\right)^2} \tag{2}$$

$$\frac{\Delta\lambda}{\lambda_0} = \frac{1}{l\pi}\arcsin\left(\frac{1-\sqrt{R_1 R_2}}{2\sqrt{R_1 R_2}}\right), l = 1, 2, 3\cdots \tag{3}$$

where R_1 and R_2 are the reflectivity of the upper and the following interfaces of the defect layer. Fig. 2(a) shows the relationship between the resonant transmittance and the reflectivity of the Bragg layers. The resonant transmittance increases with the enhancement of reflectivity of the Bragg layers. Fig. 2(b) illustrates the ratio between the linewidth of the resonant component and the resonant wavelength with the change of the reflectivity of the Bragg layers. The linewidth of the resonant component decreases as the reflectivity increases. Thus, the high transmittance and narrow linewidth can be achieved by increasing the reflectivity of the Bragg layers. In addition, it is

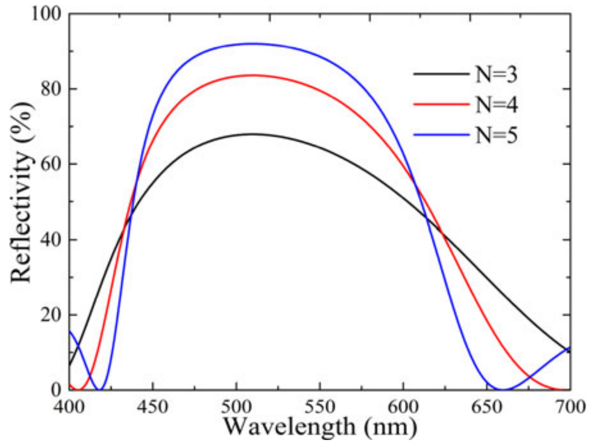

Fig. 3. Reflective spectra of the Bragg layers with different stack number of N = 3, 4, and 5.

preferred to have the same reflectivity of the Bragg layers above and below the defect layer in order to achieve high transmittance and narrow linewidth.

According to the analysis of the resonance in the defect layer, the reflectivity of the Bragg layers has significant influence over the linewidth and the transmittance of the resonant component. In the following analysis, the Bragg layers above and below the defect layer of the same structure are considered. Fig. 3 shows the reflective spectra of the Bragg layers with different stack number of N = 3, 4 and 5 when the thickness of SiO_2 and Ta_2O_5 is 96.15 nm and 62.79 nm, respectively. The reflectivity increases with the increase of the stack number. The bandwidth is inversely proportional to the stack number.

In the simulation of the proposed optofluidic filter, a commercial software Essential Macleod is used. A 1-D Bragg structure of $(Ta_2O_5/SiO_2)^N$ is calculated, in which the refractive indices of Ta_2O_5, SiO_2, and defect layer are 2.19, 1.43, and 1.5, and the thicknesses of the Ti_2O_5, SiO_2, and the defect layer are $d_H = 62.79$ nm, $d_L = 96.15$ nm, and $d_D = 380$ nm. Fig. 4(a) shows the spectra as a function of the stack number. The spectra are calculated for the stack numbers of 2, 4, and 6, respectively. The resonant components with the linewidth of 20.8 nm, 3.9 nm, and 0.84 nm are achieved. The linewidth shrinks with a negative exponential decay as the increase of the stack number, as shown in Fig. 4(b). Accordingly, an appropriate stack number is necessary to realize resonance with an expected narrow linewidth.

Fig. 4(c) shows the wavelength-dependent spectra with different defect-layer thickness when the stack number is N = 6. When the defect-layer thickness is $d_D = 130$ nm, 160 nm and 190 nm, the linewdiths are 1.96 nm, 1.65 nm and 1.55 nm, respectively. The linewidth decreases with the increase of the thickness of the defect layer as depicted in Fig. 4(d). It is worth noting that thick defect layer engenders multiple resonant peaks within the forbidden band [31] and thin defect layer might have difficulty in injection of liquid. Moreover, the sensitivity is calculated under different thickness of the defect layer.

Moreover, the sensitivity is calculated under different thickness of the defect layer. When the thickness of the defect layer is 380 nm, 350 nm and 320 nm, the shift ranges of the resonant wavelength are 12.15 nm 11.61 nm and 10.95 nm with the change of the refractive index of the defect layer from 1.4 to 1.43, which indicates that the sensitivity ($\Delta\lambda/\Delta n$) is 405 nm/RIU, 387 nm/RIU and 365 nm/RIU, respectively. Consequently, the defect-layer thickness of 380 nm is chosen.

3.2 Fabrication of Optofluidic Bragg Filter

Fig. 5 shows the fabrication procedure of the tunable optofluidic Bragg filter. The fabrication procedure has three steps: fabrication of a nanometer-thickness optical cavity with a periodic-film stack,

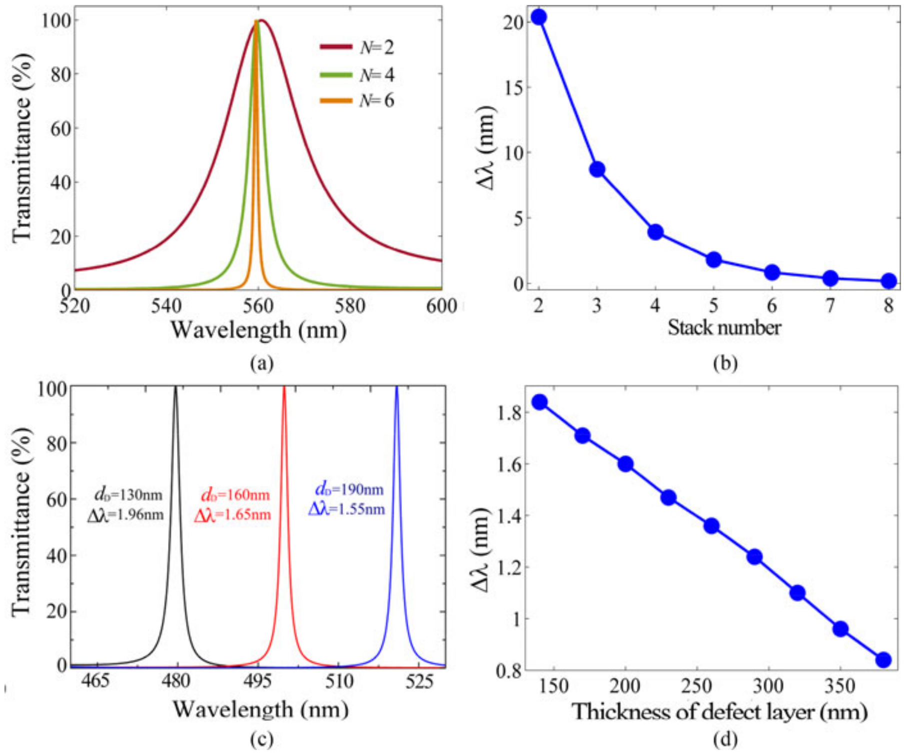

Fig. 4. (a) Spectra and (b) the linewidth versus the different stack number of the Bragg layers. (c) Spectra and (d) linewidth with different thickness of the defect-layer d_D = 130 nm, 160 nm, and 190 nm.

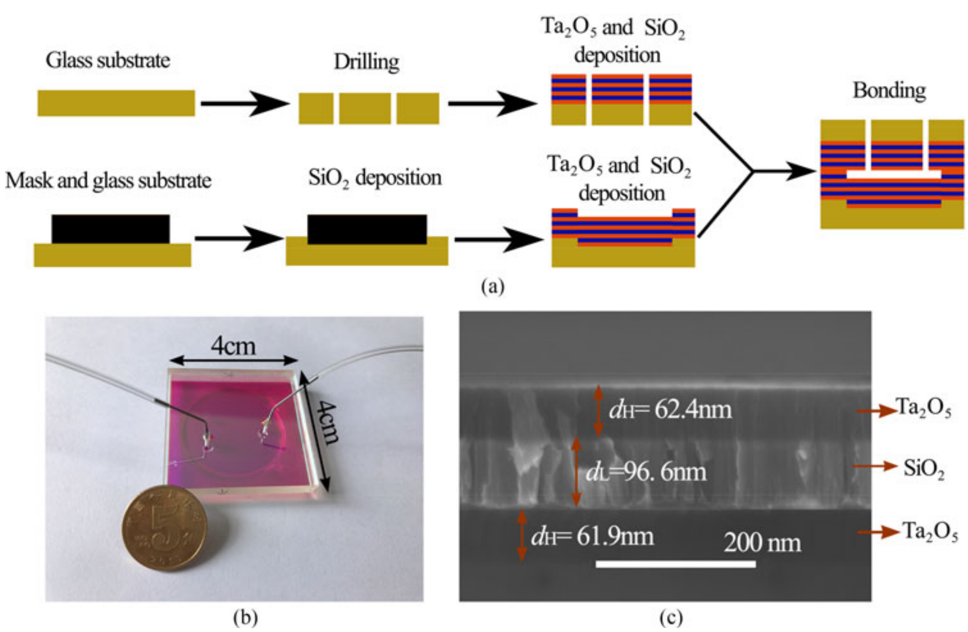

Fig. 5. (a) Fabrication procedure of the optofluidic tunable filter. (b) Optofluidic filter device and (c) the cross-section SEM image of the three-layer film. Scale bar: 200 nm.

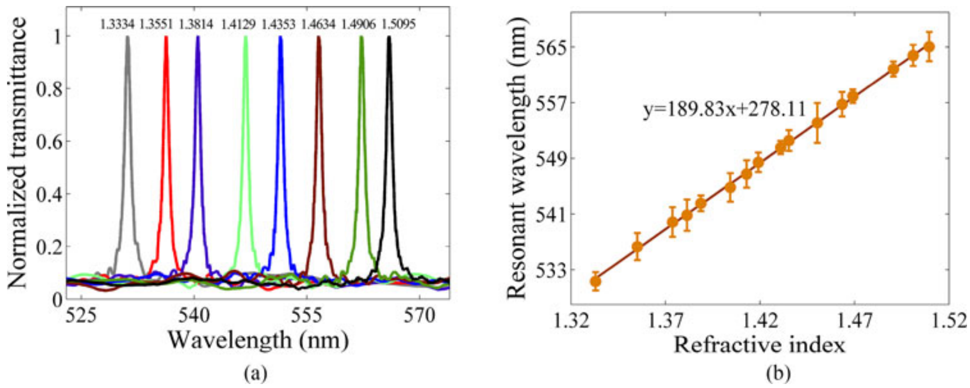

Fig. 6. (a) Measured spectra of the optofluidic Bragg filter device. (b) Resonant wavelength as a function of the refractive index of the $CaCl_2$ solution. The defect-layer has the thickness of 380 nm, and the stack number is $N = 6$.

preparation of a cover plate with two holes, and bonding of the cavity with the cover plate. First, owing to the requirement of high surface evenness of fused silica, the surface of all the fused silica plates must be precisely polished. After drilling with a punching machine, Ta_2O_5 and SiO_2 are alternately deposited on the square fused silica plate with two holes by using a sputtering system. Secondly, for fabricating the nanometer-thickness cavity with a periodic-film stack, before the nanometer-thickness SiO_2 film is deposited, a circular fused silica plate is covered by a circular glass mask of smaller size. Then, periodic films are deposited on the surface of fused silica. Finally, for bonding two fused silica plates, after the two fused silica plates are placed in close contact with each other, the sidewall of the circular fused silica plate is daubed with photosensitive gel. Because the size of the circular fused silica plate is less than that of the square plate, the photosensitive gel flows to the surface of the square plate. Finally, photosensitive gel is irradiated and solidified by ultraviolet (UV) light. The circular plate is closely adhered to the square plate. A photograph of the fabricated optofluidic tunable filter is shown in the Fig. 5(b). Fig. 5(c) shows the cross-section SEM image of three-layer film. The smooth surface and the clear layered structure can be observed. The thickness of the deposited SiO_2 and Ta_2O_5 films is 62.4 nm and 96.6 nm.

3.3 Characteristic of Optofluidic Bragg filter

To obtain solution with different refractive indices, anhydrous $CaCl_2$ of different masses is blended with deionized water. The concentration of the $CaCl_2$ solution varies from 0 to 66.7% with an increment of 0.3 g $CaCl_2$ in 6 g of deionized water. The refractive index of the solution is measured by using a refractometer (LiquiPhysics Excellence RM50). The resonant wavelength is shifted when $CaCl_2$ solution of different refractive indices is injected into the nanocavity.

In the measurement of the transmitted spectra of the tunable optofluidic Bragg filters, a tungsten-halogen lamp of wavelength ranging from 360 nm to 2000 nm was employed as a light source. Collimated light with a beam size of approximately 600 μm was incident on the tunable optofluidic Bragg filter. The spectra were measured using a spectrometer (USB2000, Ocean Optics). Fig. 6(a) shows the transmitted spectra measured with eight different refractive indices using the proposed filter. The filter has the stack number of $N = 6$ and the thickness of the defect-layer is $d_D = 380$ nm. The resonant peaks appeared at 531.1, 536.3, 540.5, 546.9, 551.5, 556.5, 562.2, and 565.9 nm when the refractive indices of the injected liquid are 1.3334, 1.3551, 1.3814, 1.4129, 1.4353, 1.4634, 1.4906, and 1.5095, respectively. The variation of the resonant wavelength is caused from the change of optical phase of the Bragg nanocavity, in which the liquid refractive index varies.

In order to validate the relationship between the resonant wavelength and the liquid refractive index, the resonant wavelength is shown in Fig. 6(b) as a function of the liquid refractive index. The error bars are standard deviation of the measured resonant wavelength in the different experimental

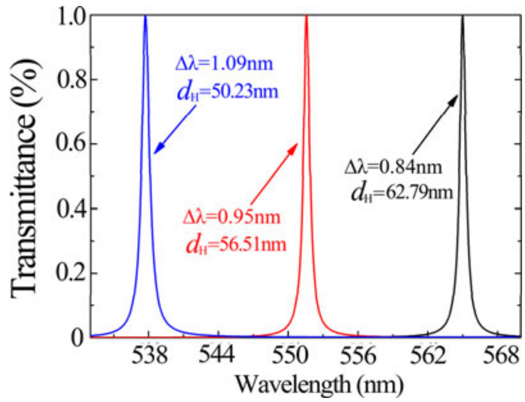

Fig. 7. Calculated spectra with different thickness of Ta_2O_5 film.

runs. It indicates that the resonant wavelength increases linearly with the increase of the liquid refractive index. The relationship between the resonant wavelength and the liquid refractive index is well fitted to a straight line expressed as $y = 189.83x + 278.11$. Meanwhile, the bandwidth is approximately 1.1 nm and a very high extinction ratio of –20.2 dB is achieved. The response time of the filter is mainly related to the stabilization of liquid pressure. In the experiment, the average response time for precise measurement is approximately 40 seconds.

Fig. 7 shows the calculated spectra when the stack number is $N = 6$ and the refractive index of the defect layer is 1.51. The thickness of Ta_2O_5 film is 50.23 nm, 56.51 nm, and 62.79 nm, respectively. The corresponding linewidth is 1.09 nm, 0.95 nm, and 0.84 nm. The extinction ratio of the calculated results is about –72.2 dB. In contrast to the experimental results, the calculated spectra have narrow linewidth and high extinction ratio. The broadening of the linewidth and the degradation of the extinction ratio in the experiment are resulted from the fabrication error such as the uniformity of the film deposition and the parallel of the Bragg layers above and below the defect layer.

4. Conclusion

In conclusion, an optofluidic linear filter based on a dielectric-film Bragg filter was designed, simulated, fabricated, and characterized. The device consists of a nanocavity sandwiched by periodic dielectric films in which the parameters are obtained using the commercial software Essentical Macleod. When the Bragg nanocavity was injected into the $CaCl_2$ solution of different refractive indices, the resonant wavelength could be linearly shifted by up to 34.8 nm. A very high extinction ratio and bandwidth of 1.1 nm were realized. The sensitivity of the refractive index ($\Delta\lambda/\Delta n$) is found to be approximately 374 nm/RIU. The proposed device has great potential for tunable optofluidic applications.

References

[1] E. Yablonovitch, "Inhibited spontaneous emission in solid-state physics and electronics," *Phys. Rev. Lett.*, vol. 58, no. 20, pp. 2059–2062, 1987.
[2] S. John, "Strong localization of photons in certain disordered dielectric superlattices," *Phys. Rev. Lett.*, vol. 58, no. 23, pp. 2486–2489, 1987.
[3] A. Mekis, J. C. Chen, I. I. Kurland, S. Fan, P. R. Villeneuve, and J. D. Joannopoulos, "High transmission through sharp bends in photonic crystal waveguides," *Phys. Rev. Lett.*, vol. 77, no. 18, pp. 3787–3790, 1996.
[4] G. Calò, A. D'Orazio, M. D. Sario, L. Mescia, V. Petruzzelli, and F. Prudenzano, "Tunability of photonic band gap notch filters," *IEEE Trans. Nanotechnol.*, vol. 7, no. 3, pp. 273–284, May 2008.
[5] H. C. Hung, C. J. Wu, and S. J. Chang, "Infrared tunable multichannel filter in a doped semiconductor-dielectric photonic crystal heterostructure," *IEEE J. Quantum Electron.*, vol. 48, no. 3, pp. 361–366, Mar. 2012.

[6] C.-J. Wu, J.-J. Liao, and T.-W. Chang, "Tunable multilayer Fabry-Perot resonator using electro-optical defect layer," *J. Electromagn. Waves Appl.*, vol. 24, no. 4, pp. 531–542, 2010.
[7] H.-C. Hung, C.-J. Wu, and S.-J. Chang, "A mid-infrared tunable filter in a semiconductor–dielectric photonic crystal containing doped semiconductor defect," *Solid State Commun.*, vol. 151, no. 22, pp. 1677–1680, 2011.
[8] J. López, L. E. González, M. Quiñonez, N. Porras-Montenegro, G. Zambrano, and M. Gómez, "Band structure of a 2D photonic crystal based on ferrofluids of $Co_{0.8}Zn_{0.2}Fe_2O_4$ nanoparticles under perpendicular applied magnetic fields," *J. Phy. Conf. Ser.*, vol. 480, no.1, 2014, Art. no. 012033.
[9] R. Ozaki, M. Ozaki, and K. Yoshino, "Defect mode in one-dimensional photonic crystal with in-plane switchable nematic liquid crystal defect layer," *Jpn. J. Appl. Phys.*, vol. 43, no. 11B, pp. L1477–L1479, 2004.
[10] X. Wang *et al.*, "Tunable Bragg filters with a phase transition material defect layer," *Opt. Exp.*, vol. 24, no. 18, pp. 20365–20372, 2016.
[11] B. Sheng, P. Chen, C. Tao, R. Hong, Y. Huang, and D. Zhang, "Linear variable filters fabricated by ion beam etching with triangle-shaped mask and normal film coating technique," *Chin. Opt. Lett.*, vol. 13, no. 12, pp. 122301–122304, 2015.
[12] C. Song, N. T. Nguyen, A. K. Asundi, and C. L. Low, "Biconcave micro-optofluidic lens with low-refractive-index liquids," *Opt. Lett.*, vol. 34, no. 23, pp. 3622–3624, 2009.
[13] J. Clausell-Tormos *et al.*, "Droplet-based microfluidic platforms for the encapsulation and screening of mammalian cells and multicellular organisms," *Chem. Biol.*, vol. 15, no. 5, pp. 427–437, 2008.
[14] C. Monat, P. Domachuk, and B. Eggleton, "Integrated optofluidics: A new river of light," *Nature Photon.*, vol. 1, no. 2, pp. 106–114, 2007.
[15] L. K. Chin, A. Q. Liu, J. B. Zhang, C. S. Lim, and Y. C. Soh, "An on-chip liquid tunable grating using multiphase droplet microfluidics," *Appl. Phys. Lett.*, vol. 93, no. 16, pp. 3332–3339, 2008.
[16] M. Hashimoto, B. Mayers, P. Garstecki, and G. M. Whitesides, "Flowing lattices of bubbles as tunable, self-assembled diffraction gratings," *Small*, vol. 2, no. 11, pp. 1292–1298, 2006.
[17] M. I. Lapsley, S.-C. S. Lin, X. Mao, and T. J. Huang, "An in-plane, variable optical attenuator using a fluid-based tunable reflective interface," *Appl. Phys. Lett.*, vol. 95, no. 95, 2009, Art. no. 083507.
[18] G. Xiao *et al.*, "A tunable submicro-optofluidic polymer filter based on guided-mode resonance," *Nanoscale*, vol. 7, no. 8, pp. 3429–3434, 2015.
[19] K. S. Chao, M. S. Lin, and R. J. Yang, "An in-plane optofluidic microchip for focal point control," *Lab Chip*, vol. 13, no. 19, pp. 3886–3892, 2013.
[20] C. Fang *et al.*, "Tunable optical limiting optofluidic device filled with graphene oxide dispersion in ethanol," *Sci. Rep.*, vol. 5, 2015, Art. no. 15362.
[21] B. S. Phillips, P. Measor, Y. Zhao, H. Schmidt, and A. R. Hawkins, "Optofluidic notch filter integration by lift-off of thin films," *Opt. Exp.*, vol. 18, no. 5, pp. 4790–4795, 2010.
[22] P. Measor, B. S. Phillips, A. Chen, A. R. Hawkins, and H. Schmidt, "Tailorable integrated optofluidic filters for biomolecular detection," *Lab Chip*, vol. 11, no. 5, pp. 899–904, 2011.
[23] E. Vasdekis and D. Psaltisa, "Optofluidic-tunable color filters and spectroscopy based on liquid-crystal microflows," *Lab Chip*, vol. 13, no. 14, pp. 2721–2726, 2013.
[24] S. Jugessur, J. Dou, and J. S. Aitchison, "Tunable optofluidic Bragg microcavity filter," *J. Amer. Vac. Soc.*, vol. 28, no. 6, pp. C608–C6010, 2010.
[25] A. S. Jugessur, J. Dou, J. S. Aitchison, R. M. De La Rue, and M. Gnan, "A photonic Bragg grating device integrated with microfluidic channels for bio-sensing applications," *Microelectron. Eng.*, vol. 86, no. 4–6, pp. 1488–1490, 2009.
[26] M. Oliva-Ramirez, L. González-García, J. Parra-Barranco, F. Yubero, A. Barranco, and A. R. Gonzalez-Elipe, "Liquids analysis with optofluidic bragg microcavities," *ACS Appl. Mater. Interface*, vol. 5, no. 14, pp. 6743–6750, 2013.
[27] P. Domachuk, I. C. M. Littler, M. Cronin-Golomb, and B. J. Eggleton, "Compact resonant integrated microfluidic refractometer," *Appl. Phys. Lett.*, vol. 88, no. 9, 2007, Art. no. 093513.
[28] L. K. Chin *et al.*, "Differential single living cell refractometry using grating resonant cavity with optical trap," *Appl. Phys. Lett.*, vol. 91, no. 24, 2007, Art. no. 243901.
[29] H. A. Macleod, *Thin-Film Optical Filters*. New York, NY, USA: Taylor & Francis, 2010.
[30] Z. Knittl, *Optics of Thin Films*. New York, NY, USA: Wiley, 1976.
[31] T.-C. King, Y.-P. Yang, Y.-S. Liou, and C.-J. Wu, "Tunable defect mode in a semiconductor-dielectric photonic crystal containing extrinsic semiconductor defect," *Solid State Commun.*, vol. 152, no. 24, pp. 2189–2192, 2012.